Stem Cell Research (2013) 11, 707–720

Available online at www.sciencedirect.com

SciVerse ScienceDirect

www.elsevier.com/locate/scr

A novel application for a 3-dimensional timelapse assay that distinguishes chemotactic from chemokinetic responses of hematopoietic CD133 $^{+}$ stem/progenitor cells

Emma E. Pepperell, Suzanne M. Watt*

Stem Cell Research Laboratory, NHS Blood and Transplant, Oxford, UK
Stem Cell Research Laboratory, Nuffield Division of Clinical Laboratory Sciences, Radcliffe Department of Medicine, University of Oxford, Oxford, UK

Received 25 November 2012; received in revised form 25 March 2013; accepted 9 April 2013
Available online 19 April 2013

Abstract Efficient homing/mobilization of human hematopoietic stem/progenitor cells to/from bone marrow niches enhances their therapeutic efficacy. Additionally, homing is dependent on cell source and may be modulated by prior ex vivo cell expansion. Here, we describe a novel application of a 3-dimensional time-lapse method for assessing trafficking of individual human cord blood CD133^{+} hematopoietic stem/progenitor cells in vitro, using the key chemokine CXCL12 as a paradigm. This new methodology allows distinction between chemotactic responses (displacement of center of mass and the forward migration index of the cells), and chemokinetic responses such as total cell path traveled in any direction (accumulated distance) and cell velocity in a 3-dimensional matrix. Other key advantages of this novel assay over existing assays include the ability to assess individual cell migration over times comparable to in vivo homing and rapid mobilization assays (18–24 h) and to directly compare the strength or response of individual hematopoietic progenitor cells to different or competing stimuli and small molecule inhibitors in a single assay prior to analyses in vivo. Importantly, using this method, our results demonstrate definitively that CXCL12 regulates the chemotactic responses of human cord blood CD133^{+} cells, but not their random migration or chemokinesis.

1. Introduction

Directed cell migration (chemotaxis) towards a stimulus is a well defined function of many mammalian and non-mammalian cells and is vital throughout embryonic and postnatal life (Petrie et al., 2009). A key example is the homing or migration of hematopoietic stem/progenitor cells (HSPCs) to specific microenvironmental niches, where their fate is determined (Bianco, 2011; Lawal and Calvi, 2011; Mazo et al., 2011; Mercier et al., 2011; Nagasawa et al., 2011; Calderón and Boehm, 2012; Park et al., 2012) or mobilization from these

* Corresponding author at: Stem Cells and Immunotherapies, NHS Blood and Transplant, John Radcliffe Hospital, Headington, Oxford OX3 9DU, UK.
E-mail address: suzanne.watt@nhsbt.nhs.uk (S.M. Watt).

1873-5061
http://dx.doi.org/10.1016/j.scr.2013.04.006

niches using small molecule strategies or in disease states (Kolonin and Simmons, 2009; Shiozawa and Taichman, 2010; Mohty and Ho, 2011; Psaila et al., 2012). Importantly, in the clinical setting, prior manipulation or expansion of HSPCs can compromise or enhance their homing or migratory capacities and this can affect transplant outcomes (Aljitawi, 2012). This is particularly pertinent for cord blood where HSPC content is limited, engraftment and hematological reconstitution are delayed compared to bone marrow or mobilized peripheral blood, one cord blood unit will engraft in preference to another in double cord blood transplants, and expansion/manipulation ex vivo prior to transplant is used to reduce delayed engraftment (Dahlberg et al., 2011; Nagasawa et al., 2011; Petropoulou and Rocha, 2011; Watt, 2011; Aljitawi, 2012; Broxmeyer, 2012; Christopherson et al., 2012; Csaszar et al., 2012; Ramirez et al., 2012).

The CXC chemokine, CXCL12, is a key chemo-attractant for HSPC homing to bone marrow, also regulating HSPC motility, homing to, and retention, survival, and proliferation in this niche (Peled et al., 1999; Dar et al., 2006; Watt and Forde, 2008; Sharma et al., 2011; Bonig and Papayannopoulou, 2013). The cognate receptors for CXCL12 are CXCR4 and CXCR7, although the latter is poorly expressed on human HSPCs (Hartmann et al., 2008; Sun et al., 2010). However, where expressed on other cells, CXCR7 is thought to act as a decoy receptor or co-receptor for CXCR4 (Naumann et al., 2010; Sun et al., 2010). CXCL12/CXCR4 deficient mice demonstrate defects in hematopoietic, immune, circulatory and central nervous systems (Zou et al., 1998; reviewed in Watt and Forde, 2008). Co-operation and cross talk between CXCL12/CXCR4, other receptors/proteins, and signaling molecules are thought to fine tune cellular responses and/or specificity for microenvironmental niches (Forde et al., 2007; Christopherson et al., 2012; Schiraldi et al., 2012).

The gold standard for determining efficient HSPC homing to bone marrow niches is their subsequent hematological reconstitution following transplantation in humans (Dahlberg et al., 2011; Ramirez et al., 2012), or, as surrogates, in immunodeficient mice or non-human primates (Goessling et al., 2011; Larochelle et al., 2012). Similar models are used to assess the efficacy of mobilizing agents (Hoggatt and Pelus, 2011; Bonig and Papayannopoulou, 2013). However, surrogate assays are time consuming and costly and do not discriminate between direct effects on HSPCs nor indirect mechanisms mediated by bone marrow niche elements. An initial homing/migration assay ex vivo, which reduces animal usage and allows refinement of pre-transplant protocols would make screening of expansion/manipulation/mobilization protocols more efficient and provide essential insights into mechanisms. Although current transwell migration end-point assays (Toetsch et al., 2009) measure cell migration towards CXCL12, these simply give a percentage of cells migrating across a membrane towards a stimulus.

We have developed a novel reproducible in vitro homing/migration assay using 3D μ-slide chemotaxis chambers from Ibidi GmbH and timelapse microscopy to track individual human HSPCs and have used CXCL12 as a paradigm. This allows the user to compare chemotactic and chemokinetic effects of a stimulus on HSPC homing/migration, as well as observing individual cells during the migratory process. Importantly, using this new methodology, we have definitively demonstrated, in contrast to previous assumptions that chemokines alter both chemotactic and chemokinetic responses simultaneously (Entschladen et al., 2005), that CXCL12 regulates human umbilical cord blood (UCB) $CD133^+$ HSPC chemotaxis but not chemokinesis. Furthermore, we use this assay to compare the chemotactic and chemokinetic responses of UCB $CD133^+$ cells after an 8 day expansion on a cell-free nanofiber scaffold in defined cytokine cocktails.

2. Materials and methods

2.1. Cell collection, isolation and culture

Human UCB units were collected with written informed pre-consent and ethical approval from Oxford and Berkshire National Research Ethical Committees, and studies conducted with approval of the NHSBT research committee. Mononuclear cells from individual or pooled UCB units were isolated by density gradient centrifugation on lymphocyte separation medium 1077 (PAA Laboratories, Pasching, Austria; density < 1.077 g/ml) (Forde et al., 2007) before CD133 immunomagnetic bead selection (Miltenyi Biotec, Bergisch Gladbach, Germany) (Forde et al., 2007). Cell purity was assessed by flow cytometry (Forde et al., 2007; Zhou et al., 2012). In nonexpansion experiments, pooled or individual freshly harvested or cryopreserved $CD133^+$ cells were cultured at 5×10^5 cells/ml in StemSpan serum-free medium (Stem Cell Technologies, Grenoble, France) containing 100 ng/ml interleukin-6 (IL-6), 20 ng/ml thrombopoietin (TPO), 100 ng/ml stem cell factor (SCF), and 100 ng/ml FLT3 ligand (R&D Systems, Minneapolis, MN, USA) in 6–12 well tissue culture plates at 37 °C for 24 h prior to use (Forde et al., 2007).

2.2. Flow cytometry

$CD133^+$ cells were incubated with FcR block and the relevant antibodies (mouse (m) anti-human PE- or APC-CD133/2 (293C3), APC- or PerCP-CD34 (AC136 or 8G12 respectively) (all from Miltenyi Biotec), APC- or PeCy5-CXCR4 (12G5; BD Biosciences, San Jose, CA, USA), APC-CD45 (HI30; BD Biosciences), or relevant isotype controls (PE- or APC-mIgG2b-PE, APC- or PerCP-mIgG2a (Miltenyi Biotec), APC- or PeCy5-mIgG2a or APC-mIgG1-APC (BD Biosciences)) Forde et al., 2007; Zhou et al., 2012), DAPI (1:50,000 dilution, Invitrogen Ltd., Paisley, Scotland) was added as a viability stain before cells were analyzed on a BD LSR II flow cytometer using the BD FACSDiva 6 software program (both from BD Biosciences) (Forde et al., 2007; Zhou et al., 2012).

2.3. Expansion of human UCB $CD133^+$ cells

Nanex nanofiber plates (Arteriocyte Inc., Cleveland, Ohio, USA) were kindly provided by or purchased from Cambridge Bioscience (Cambridge, England) and used as the scaffold to expand human UCB $CD133^+$ cells. The conditions developed by Arteriocyte (Nanex HSC serum free expansion media with the undisclosed Nanex cytokines) were defined as standard Nanex conditions. Other conditions used were the Nanex HSC expansion media with 100 ng/ml SCF, Flt-3 ligand, IL-6 and 20 ng/ml TPO (R&D Systems; defined as Nanex with SCF, Flt-3 ligand, IL-6 and TPO), and Nanex HSC expansion media

with 100 ng/ml IGFBP2 (R&D Systems) and Angptl5 (Miltenyi Biotec) as well as 100 ng/ml SCF, Flt-3 ligand, IL-6 and 20 ng/ml TPO (defined as Nanex with IGFBP2 and Angptl5). UCB CD133$^+$cells freshly isolated as above or used after cryopreservation were suspended in Nanex medium without cytokines for 4 h before seeding onto the Nanex nanofiber plates (3×10^3 cells/3 ml in 6 well Nanex plates) in specified media. After 8 days in culture, cells were collected by pipetting and a 1 min trypsinization prior to determining viable total nucleated cell (TNC) counts and the proportions of CD133, CD34 and CD45 positive cells. After expansion, CD133$^+$ cell double re-purification was carried out using CD133$^+$ immunomagnetic beads as above, the purity assessed by flow cytometry and the chemotactic and chemokinetic ability of the re-purified cells determined using the 3D μ-slide chemotaxis assay described below.

2.4. Final chemotaxis assay

The 3D chemotaxis μ-slide (Ibidi GmbH, Munich, Germany), StemSpan media (Stem Cell Technologies) and beveled pipette tips (Grenier Bio-One, GmBH Frickenhausen, Germany) were pre-equilibrated for 24 h in a 37 °C incubator. After culture, UCB CD133$^+$ cells were washed in StemSpan media to remove cytokines and re-suspended at 3×10^5 cells/100 μl in cold bovine collagen I gel solution, comprising 20% (v/v) bovine collagen I gel (5 mg/ml) in α-MEM medium (both from Invitrogen Ltd.). Six microliter of the collagen gel containing cell suspension was quickly seeded into the central chamber (the observation area) of the 3D chemotaxis μ-slide (Fig. 1A(a)). The slide was then covered with the lid, and incubated in a humidified incubator at 37 °C upside-down for 1 h until the collagen I gel had set. The reservoirs either side of the observation chamber were then filled slowly using a beveled pipette tip with up to 70 μl serum free StemSpan media (control media; Stem Cell Technologies) or chemoattractant media comprising StemSpan media plus CXCL12 (Peprotech, tebu-bio, Peterborough, England) in order to establish a CXCL12 gradient over the observation area (Fig. 1A(b)). Where appropriate, the small molecule CXCR4 antagonist, AMD3100 (Sigma-Aldrich Co. Ltd., Gillingham, England), was added to these reservoirs. The filling channels were plugged to prevent evaporation and the slide(s) secured on a Prior Proscan II controlled motorized stage in a 37 °C humidified heat chamber surrounding the Nikon Eclipse TE300 microscope (Nikon UK Ltd., London, England).

2.5. Data capture and analyses

Data were captured with a Hamamatsu ORCA-ER camera using SimplePCI automated image capture camera device software (Hamamatsu Photonics UK Ltd., Welwyn Garden City, England). Cell migration was imaged by timelapse microscopy (Nikon Eclipse TE300 microscope) and photographs taken at regular intervals (3–5 min) at ×4 magnification for up to 22 h. The data were exported as multipage TIFF files to enable manual cell tracking using the Image J 'Manual Tracking' plug-in (rsbweb.nih.gov/ij/; Ibidi GmbH) and the Image J 'Chemotaxis and Migration Tool' plug-in (Ibidi GmbH) used to quantitate data. The first frame of the movie (time point 0) was printed and 45–50 cells were selected randomly before visualizing the entire movie sequence throughout the observation chamber. These selected cells were then tracked individually again in random order until a minimum of 30 viable cells, which did not divide during the experiment, had been tracked. Experiments were repeated between 3 and 8 times. The software was also used to derive trajectory plots (Fig. 1B) and to quantify the various chemotactic or chemokinetic responses (Fig. 1C) including i) accumulated distance (total cell path traveled), ii) Euclidean distance (the shortest distance between cell start and end points), iii) displacement of the center of mass (COM; average end position of tracked cells), iv) directionality (the ratio between Euclidean distance and accumulated distance or the straightness of the path), v) forward migration index (FMI; the ratio between the net distance traveled on the relevant axis and the accumulated distance), and vi) cell velocity.

2.6. Optimizing the chemotaxis assay

Human UCB CD133$^+$ cells were cultured in serum free StemSpan media (Stem Cell Technologies) containing 100 ng/ml SCF, Flt-3 ligand, IL-6 and 20 ng/ml TPO (R&D Systems) for 24 h (Forde et al., 2007) and then washed in StemSpan medium before commencing the 3D μ-slide chemotaxis assay as described above. In optimizing the migration conditions for UCB CD133$^+$ cell chemotaxis, different collagen I concentrations (0.5, 1 or 3 mg/ml collagen I gels), different CXCL12 concentrations (0, 0.2, 1 or 2 μg/ml CXCL12), different timepoints (4, 10, 18 and 22 h), different AMD3100 concentrations (0, 1 and 10 μM) and pooled versus non-pooled UCB CD133$^+$ cells were tested.

2.7. Statistical analysis

As the data were non-parametric, as determined using the Shapiro–Wilk and D'Agostino and Pearson omnibus normality tests and the F test to compare variances (Prism, GraphPad Software Inc., La Jolla, CA, USA), the Mann Whitney test was used to determine if significant where appropriate. When data parameters were correlated, using paired data from independent experiments, the line was fitted using linear regression and the Spearman's rank test was used to determine the correlation coefficient using Prism software (www.graphpad.com/prism/prism.htm). The r_s value displayed the goodness of fit, while the p value determined whether the slope was significantly different from 0. For the chemotaxis assay, the Rayleigh test was used to assess if data were significantly inhomogeneously distributed in any direction when p was <0.05. Unless otherwise stated, raw data and median or means and SEM are shown for $n \geq 3$ independent experiments and with $^*p < 0.05$, $^{**}p < 0.01$, and $^{***}p < 0.001$ being significant to highly significant.

3. Results

3.1. Optimization and validation of the 3D μ-slide chemotaxis assay for human UCB CD133$^+$ cells

To establish and validate the 3D μ-slide chemotaxis assay, freshly isolated or cryopreserved and thawed human UCB CD133$^+$ HSPCs cultured for 24 h prior to use in serum free media containing SCF, Flt-3 ligand, IL-6 and TPO were analyzed

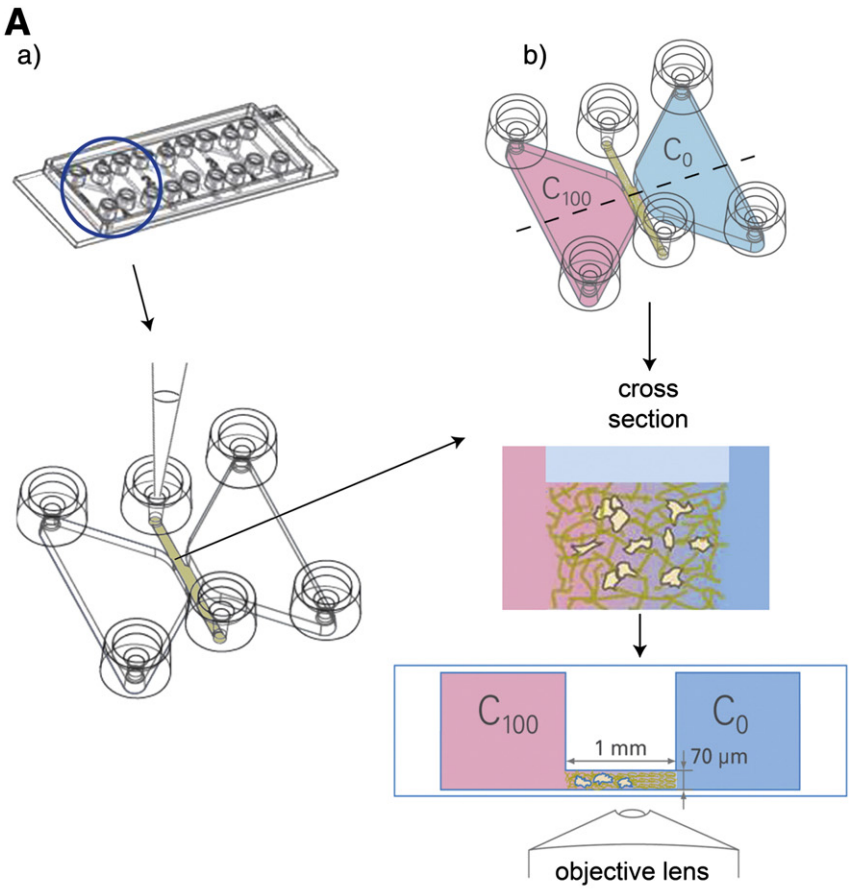
A
a)
b)
C100
C0
cross
section
C100
C0
1 mm
70 µm
objective lens

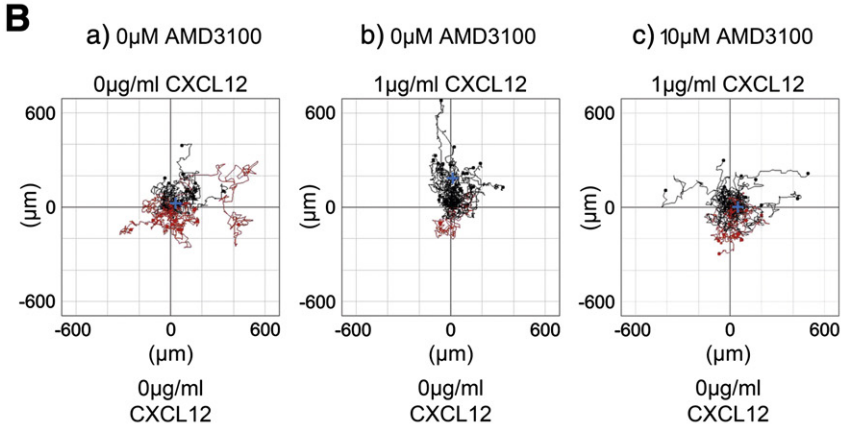
B
a) 0µM AMD3100
b) 0µM AMD3100
c) 10µM AMD3100
0µg/ml CXCL12
1µg/ml CXCL12
1µg/ml CXCL12
600
0
-600
(µm)
0µg/ml
CXCL12

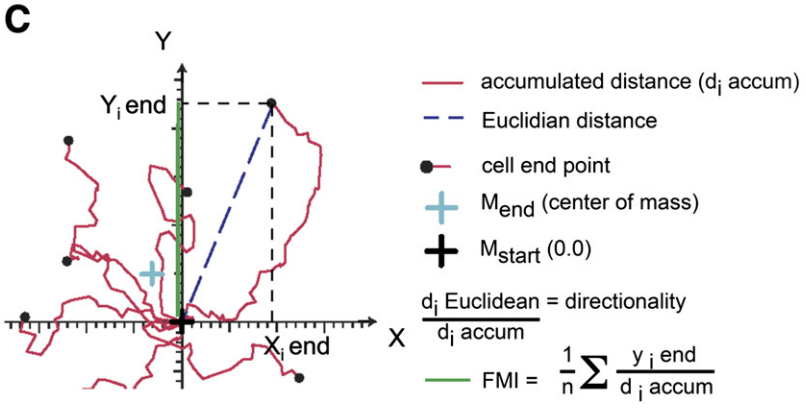
C
Y
Yi end
X
Xi end
accumulated distance (di accum)
Euclidian distance
cell end point
Mend (center of mass)
Mstart (0.0)
di Euclidean / di accum = directionality
FMI = 1/n Σ yi end / di accum

for their chemotactic and chemokinetic abilities. Following culture, cells were 94.0% ± 2.0 CD133$^+$, and essentially all expressed cell surface CXCR4 (Supplementary Fig. 1).

3.1.1. Matrix, chemokine concentration and timecourse optimization

To optimize the chemotactic protocol, 4 variables were examined: i) the need for and composition of the 3D matrix, ii) the CXCL12 concentration, iii) timecourse of migration, and iv) the use of pooled vs. individual cord blood units. As migration could not be optimized without a 3D matrix to hold the CD133$^+$ cells, we tested 3 matrices, matrigel, methylcellulose and collagen I. Neither matrigel nor methylcellulose proved practical for this application. In contrast, collagen I gels (0.5 to 3 mg/ml) supported CD133$^+$ cell movement as illustrated by their accumulated distance and velocity (Fig. 2A(a,b)). Significant chemotaxis was observed for all gel concentrations ($p < 0.05$, Rayleigh test). Chemotactic migration towards CXCL12 was on average slightly, although not significantly ($p > 0.05$), higher with the 3 mg/ml collagen I gel, but more variable when compared with 0.5 or 1 mg/ml collagen I gels as illustrated for the displacement of the center of mass (153.6 μm ± 49.0 versus 94.6 μm ± 19.0 and 113.7 μm ± 1.1 respectively) (Fig. 2A(c)). Chemokinetic migration was on average lower with the 3 mg/ml collagen I gel, but more variable when compared with 0.5 or 1 mg/ml collagen I gels as illustrated for the accumulated distance (916 μm ± 276 versus 1030 μm ± 150 and 1159 μm ± 146 respectively) (Fig. 2A(a)) and for the velocity (0.66 μm/min ± 0.20 versus 0.82 μm/min ± 0.10 and 0.92 μm/min ± 0.10 respectively) (Fig. 2A(a)). This variability resulted from a lack of uniformity in the collagen fiber formation at 3 mg/ml concentrations due to the speed at which the gel set when less diluted (Fig. 2B). This was further exemplified when comparing the ranges in the forward migration index, displacement of the center of mass, accumulated distance and velocity (Fig. 2A(c,d)). As 1 mg/ml collagen I gel showed least variability amongst independent experiments and consistently retained the cells while permitting cell movement, this matrix and concentration were chosen for our experiments.

The concentration of CXCL12 was optimal at 1 μg/ml CXCL12, as illustrated for the displacement of center of mass and the forward migration index (Figs. 3A and B(a,b)). Interestingly, there was no difference in cell velocity or accumulated cell distance with increasing concentrations of CXCL12 (between 0 to 2 μg/ml), indicating that human UCB CD133$^+$ cell chemokinesis is not influenced by the presence of CXCL12 (Fig. 3B(c,d)).

When migration was examined as a function of time, the displacement of the center of mass of CD133$^+$ cells exposed to CXCL12 increased linearly over 4–18 h before beginning to plateau (Figs. 4A and B(f)). The forward migration index of cells in the presence of CXCL12 plateaued between 4 and 10 h (Fig. 4B(h)). While the accumulated distance increased linearly over time, the largest increase in cell velocity occurred during the first 4 h of the assay (0 to 0.71 ± 0.14 μm/min). The accumulated distance and velocity increases observed for the CD133$^+$ cells over time were independent of a CXCL12 gradient (Fig. 4B(a to d)). CD133$^+$ cell migration towards CXCL12 in the 3D μ-slide assay was compared for pooled or individual cord blood units, and although individually variable, no significant difference in the median chemotactic or chemokinetic measures was observed (Supplementary Fig. 2).

3.1.2. CXCL12 influences human UCB CD133$^+$ cell chemotaxis but not chemokinesis

The final validated procedure (Fig. 1) unless otherwise specified involved culturing human UCB CD133$^+$ cells for 24 h in StemSpan serum-free medium with SCF, Flt-3 ligand, IL-6 and TPO, washing to remove cytokines and re-suspending cells at 3×10^5 cells/100 μl in a cold collagen I gel prior to seeding onto the observation area of 3D μ-slide and adding 0 or 1 μg/ml CXCL12 to opposing reservoirs. Then, each chamber was photographed at 3–5 min intervals using timelapse microscopy for up to 22 h. Supplementary Movie 1 shows representative trajectory plots of the chemotactic response of 30 randomly selected individual UCB CD133$^+$ HSPCs towards 1 μg/ml CXCL12 over 22 h. Fig. 5A(a–c) illustrates a significant difference over 8 independent experiments in chemotaxis towards CXCL12 (1 μg/ml) versus 0 μg/ml CXCL12 as determined by the Rayleigh test, displacement of center of mass and forward migration index. Individual experimental p values as determined by the Rayleigh test were between 6×10^{-3} to 6×10^{-9} with CXCL12 and 0.16 to 0.69 without CXCL12. Interestingly, there was no significant difference in cell velocity (1.0 μm/min ± 0.1 vs 1.1 μm/min ± 0.1) or accumulated distance (1258 μm ± 94 vs 1389 μm ± 91) with or without CXCL12 (Fig. 5A(e,d)), indicating that CD133$^+$ cell chemokinesis is not influenced by the presence of CXCL12.

The different parameters were compared to each other using a Spearman's rank correlation analysis to ensure that the measures used were valid and accurately represented the movement of the cells. Forward migration index and displacement of the center of mass were highly correlated (Fig. 5B(a)). Directionality and forward migration index were also highly correlated as the forward migration index measures overall chemotactic efficiency, and directionality the straightness of the cell path (Fig. 5B(b)). Similarly, displacement of the center of mass correlated with directionality (Fig. 5B(c)). Velocity and accumulated distance were highly correlated as the further the

Figure 1 The 3D μ-slide chemotaxis assay for human cord blood CD133$^+$ hematopoietic stem/progenitor cells. (A) After 24 hour culture in StemSpan medium plus SCF, Flt-3 ligand, IL-6 and TPO, (a) human UCB CD133$^+$ cells in a collagen I gel solution (1 mg/ml) were seeded into the central 3D μ-slide chamber prior to (b) the addition of StemSpan serum free medium alone (C0) or with a 1 μg/ml CXCL12 (C100) gradient plus or minus AMD3100 and cells captured by timelapse microscopy at 3–5 minute intervals. (B) Trajectory plots illustrate migrated cells at 22 h minus (a) or plus a CXCL12 gradient (b) or with CXCL12 in the presence of 10 μM AMD3100 (c). The red and black lines indicate whether the cells finished their migration path below or above their starting point on the x axis. Rayleigh test p values of $p = 0.17$, $p = 5.7 \times 10^{-8}$ and $p = 0.054$ for (a), (b) and (c) respectively indicate that the distribution of the cell end points was only significantly inhomogeneous (i.e. distributed towards the chemoattractant) in the presence of CXCL12 alone (b). (C) Diagrammatic representation of a trajectory plot demonstrating methods for quantitating chemotactic and chemokinetic parameters. The diagrams in Figs. 1A and C were captured from the movie describing the assay system (MV_25_chemotaxis.flv) on the Ibidi website (http://ibidi.com/support/movies/mv25/).

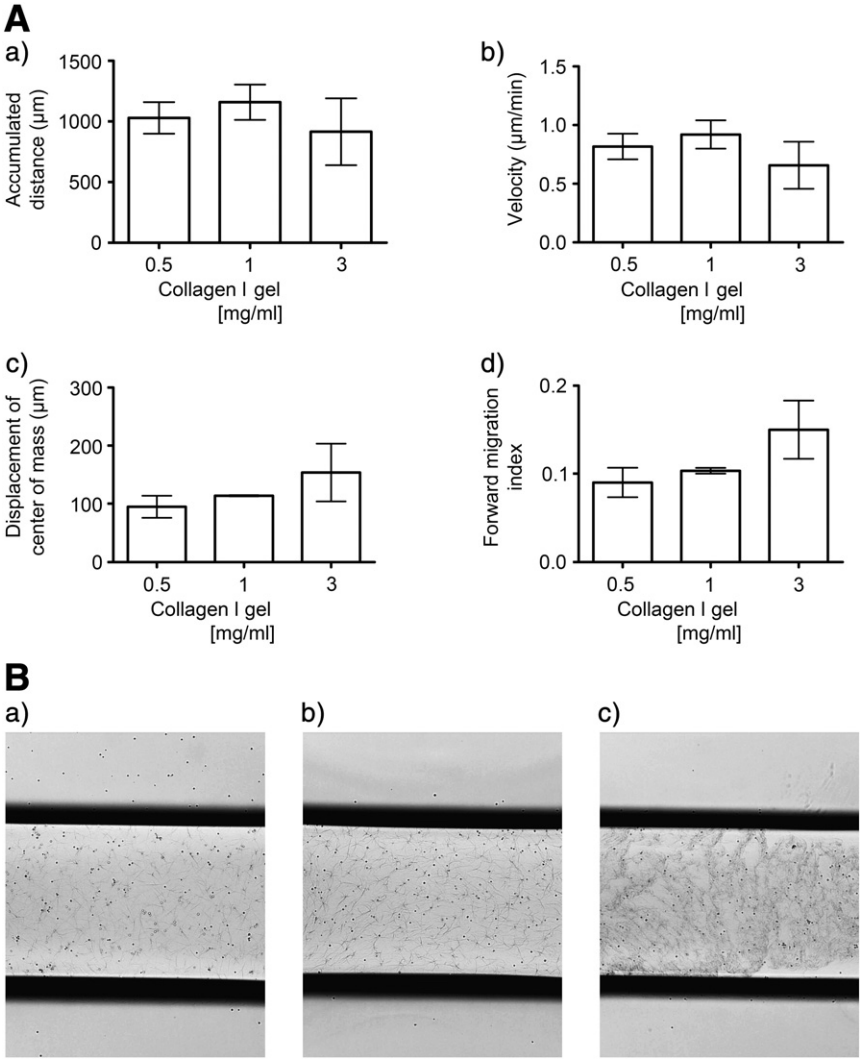

Figure 2 The effects of collagen I gel concentrations on CD133$^+$ cell migration in the 3D µ-slide assay. (A) After 24 hour culture of human UCB CD133$^+$ cells in StemSpan medium and SCF, Flt-3 ligand, IL-6 and TPO, cells were suspended in 0.5 mg/ml, 1 mg/ml or 3 mg/ml collagen I gel solutions and seeded into the central chamber of the 3D chemotaxis µ-slides. A chemokine gradient was established using 1 µg/ml CXCL12. The cells were imaged over 22 h by timelapse microscopy migration and analyzed using Image J manual tracking software and the chemotaxis and migration tool plug in for (a) accumulated distance, (b) velocity, (c) displacement of the center of mass and (d) forward migration index. Values are means ± SEM (n ≥ 3independent experiments). Variability amongst independent experiments was increased when 3 mg/ml collagen I gels were compared with 0.5 or 1 mg/ml collagen I gels. This is exemplified when comparing 1 mg/ml and 3 mg/ml collagen I gels respectively for the ranges in the accumulated distance (1012 µm to 1451 µm vs. 350 µm to 1467 µm respectively), velocity (0.77 to 1.16 vs. 0.27 to 1.18 µm/min respectively), displacement of center of mass (111.80 to 115.43 vs. 26.94 to 256.20 µm respectively) and forward migration index (0.100 to 0.110 vs. 0.060 to 0.220 respectively). (B) Microscopic images (×4 magnification) of CD133$^+$ cells in (a) 0.5 mg/ml, (b) 1 mg/ml and (c) 3 mg/ml collagen 1 gels after seeding into the central chamber of the 3D chemotaxis µ-slide and demonstrating the lack of uniformity of collagen I fibers with 3 mg/ml collagen I gels.

faster the cells move, the further they travel in the given time (Fig. 5B(d)). A negative, highly significant correlation was observed between the p values for the Rayleigh test and both the displacement of center of mass and forward migration index (Fig. 5B(e,f)). This confirmed that the Rayleigh test was a useful tool for defining chemotaxis, as the greater the displacement of center of mass or forward migration index, the more significant the p value. No significant correlations were seen between the displacement of the center of mass and velocity or accumulated distance. Neither was there any correlation between p values from the Rayleigh test and velocity or accumulated distance.

3.2. AMD3100 blocks CD133$^+$ cell chemotaxis but not chemokinesis of human UCB CD133$^+$ cells

To demonstrate that migration could be modulated by specific small molecule inhibitors, the CXCR4 antagonist AMD3100 (Goessling et al., 2011) was added to the 3D µ-slide

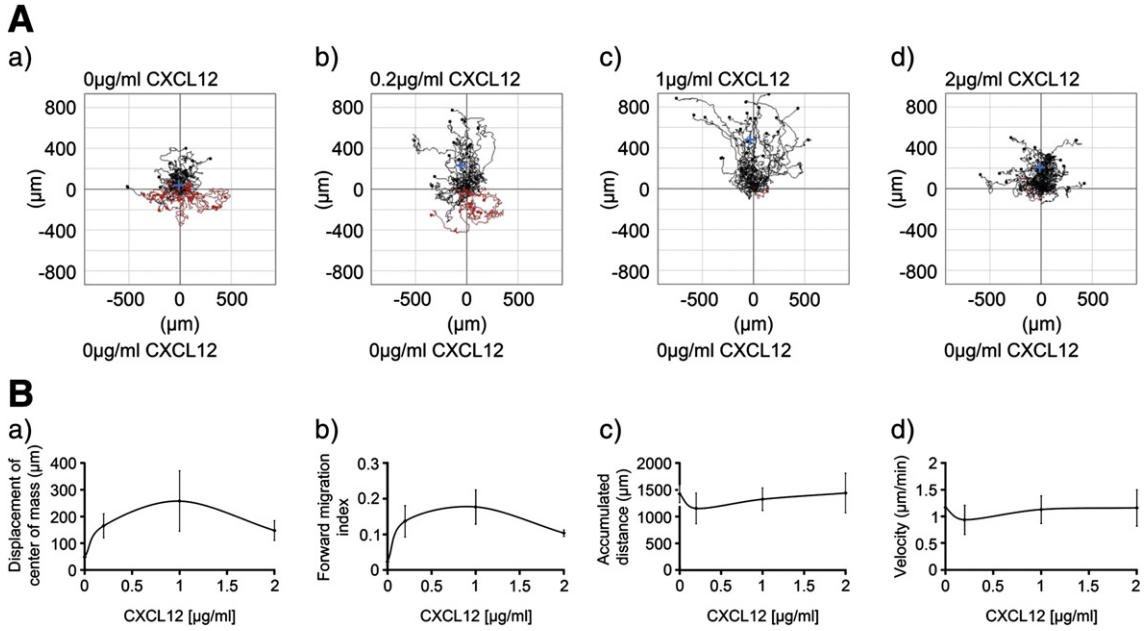

Figure 3 The CD133+ cell chemotactic response to increasing concentrations of CXCL12. Human UCB CD133+ cells cultured in StemSpan medium with SCF, Flt-3 ligand, IL-6 and TPO for 24 h were encapsulated in 1 mg/ml collagen I gel and seeded into the central chamber of the 3D chemotaxis μ-slides. 0 μg/ml, 0.2 μg/ml, 1 μg/ml or 2 μg/ml CXCL12 were added to create a chemokine gradient. The cells were imaged over 22 h by timelapse microscopy and analyzed using Image J manual tracking software and the chemotaxis and migration tool plug-in. (A) Representative trajectory plots after CD133+ cells were exposed to differing concentrations of CXCL12. The red and black lines indicate whether the cells finished their migration path below or above (towards differing CXCL12 concentrations) their starting point on the x axis. Rayleigh test p values were $p = 0.16$, $p = 6.1 \times 10^{-5}$, $p = 4.0 \times 10^{-10}$ and $p = 1.0 \times 10^{-7}$ respectively for figures (a)–(d) indicating that the distribution of the cell end points was only significantly inhomogeneous (i.e. distributed towards the chemoattractant) in the presence of CXCL12 (b)–(d) and that this was most significant with 1 μg/ml (c). (B) shows the quantitative data for (a) displacement of center of mass (257.8 μm ± 112.9 for 1 μg/ml compared to no CXCL12 of 48.8 μm ± 8.9), (b) forward migration index (0.18 ± 0.05 for 1 μg/ml compared to no CXCL12 of 0.02 ± 0.00), (c) cell velocity and (d) accumulated distance as a function of CXCL12 concentration. Values are means ± SEM for n = 3 independent experiments.

chemotaxis reservoir and shown to be inhibitory (Fig. 6). With CXCL12 and no AMD3100, the p values for the Rayleigh test were significant ($p < 0.01$ for all experiments), however with addition of 1 μm and 10 μm AMD3100, they were not significant ($p > 0.05$; Fig. 6(e)). With AMD3100 addition, there was a significant decrease in the displacement of the center of mass and forward migration index towards CXCL12 (Fig. 6(a,b); Supplementary Movies 1–3). Interestingly, there was no reduction in chemokinesis in terms of the accumulated distance nor cell velocity in the presence of CXCL12 without AMD3100 or in the presence of 1 μM or 10 μM AMD3100 (Fig. 6(c,d)).

3.3. Expanded human UCB CD133+ cells retain their chemotactic response towards CXCL12

In Supplementary Fig. 3, we demonstrate using Nanex nanofiber scaffolds in serum free Nanex medium that SCF, Flt-3 ligand, IL-6 and TPO promoted a 65 ± 4 fold expansion of freshly isolated human UCB CD133+ HSPCs. We therefore compared the effects on CD133+ cell chemotaxis of expanding identical aliquots of human UCB CD133+ cells in such cultures (this time after cryopreservation and thawing) containing SCF, Flt-3 ligand, IL-6 and TPO without or with the addition of 100 ng/ml IGFBP2 and 100 ng/ml Angptl5. Cells before expansion were 88.4% ± 2.8 CD133+, 96.5% ± 3.0 CD45+ and 93.8% ± 2.6 CD34+. After 8 days of culture, the expanded cells without and with IGFBP2 and Angptl5 were respectively 85.0% ± 4.3 and 86.6% ± 3.0 viable, 96.8% ± 3 and 96.6% ± 3.3 CD45+, and 38.7% ± 10.2 and 37.7% ± 9.7 CD34+CD133+ (Fig. 7A(a)). Total nucleated cell (TNC) expansion was 148 ± 49 and 209 ± 64 fold for the cells cultured with SCF, Flt-3 ligand, IL-6 and TPO without or with IGFBP2 and Angptl5 respectively (Fig. 7A(b)), while CD34+ cell expansion was 107 ± 46 and 147 ± 61 fold respectively (Fig. 7A(b,c)). Although there was some variability in the TNC and CD34+ cell expansion in three independent experiments, CD133+ cell expansion was more consistent amongst experiments (Fig. 7A(b,c)). There was a 52 ± 6 and 73 ± 6 fold increase in CD133+ cells and a 52 ± 4 and 73 ± 2 fold increase in CD133+CD34+ cells without and with IGFBP2 and Angptl5 respectively (Fig. 7A(b,c)). Thus, the addition of IGFBP2 and Angptl5 enhanced CD133+ and CD34+CD133+ cell numbers approximately 1.5 fold over 8 days.

The cultured human UCB CD133+ cells were assessed for their ability to migrate to CXCL12 using the 3D μ-slide chemotaxis assay. After CD133+ cell purification, CD133+ cell purities were respectively 92.8% ± 3.3 and 94.5% ± 1.2 (Fig. 7B(c,d)) and recoveries were respectively 51.8% ± 9.9 and 43.8% ± 12.8 for cells expanded in Nanex media with SCF, IL-6, TPO and Flt-3 ligand without or with IGFBP2 and Angptl5. CXCR4 expression was present on essentially all CD133+ cells (Fig. 7B(g,h)). Figs. 7C and D demonstrate an enhanced

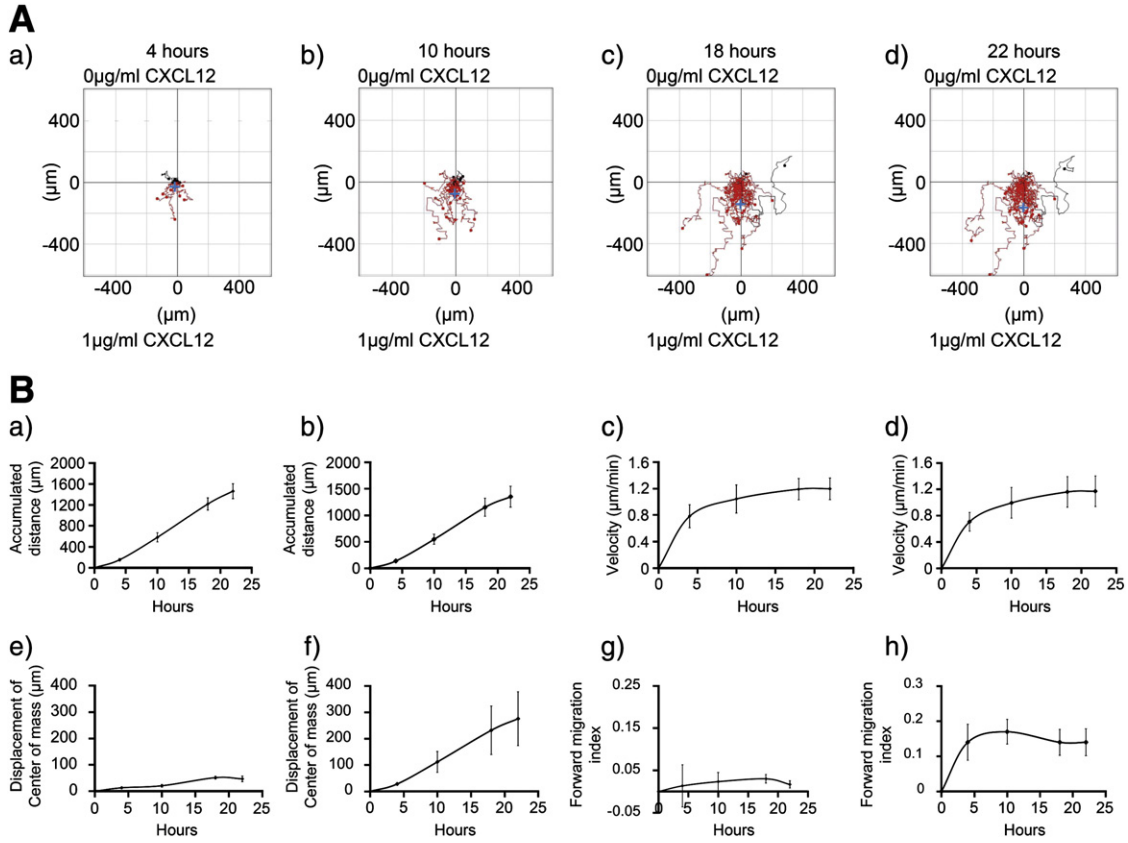

Figure 4 CD133$^+$ cell chemotaxis and chemokinesis as a function of time. Human UCB CD133$^+$ cells were cultured in StemSpan medium with SCF, Flt-3 ligand, IL-6 and TPO for 24 h, encapsulated in 1 mg/ml collagen I gel and seeded into the central chamber of the 3D chemotaxis µ-slides, prior to adding 0 µg/ml or 1 µg/ml CXCL12 to form a chemokine gradient as illustrated in Fig. 1. Cell migration was imaged for 22 h by timelapse microscopy and tracked and analyzed using Image J manual tracking software and the chemotaxis and migration tool plug-in after 4, 10, 18 and 22 h. (A) shows representative trajectory plots (a) 4 h, (b) 10 h, (c) 18 h and (d) 22 h (the blue cross shows the displacement of the center of mass) of cells exposed to 1 µg/ml CXCL12. The red and black lines indicate whether the cells finished their migration path below (towards 1 µg/ml CXCL12) or above their starting point on the x axis. The Rayleigh test indicate that the distribution of the cell end points was significantly inhomogeneous at all time points (i.e. distributed towards the chemoattractant) in the presence of CXCL12 ($p = 4.0 \times 10^{-3}$, $p = 2.9 \times 10^{-5}$, $p = 6.7 \times 10^{-7}$ and 2.0×10^{-8} for (a)–(d) respectively. (B) shows the quantitative data for (a,b) accumulated distance, (c,d) velocity, (e,f) displacement of the center of mass, and (g,h) forward migration index, of cells exposed to 0 µg/ml CXCL12 (a,c,e,g) or 1 µg/ml CXCL12 (b,d,f,h) respectively. Values are means ± SEM for n = 3 independent experiments.

chemotactic response towards CXCL12 when additionally stimulated with Angptl5 and IGBP2 (although not reaching statistical significance in 3 experiments), and no significant change in chemokinetic responses ($p > 0.5$). Thus, the expansion did not compromise CD133$^+$ cell chemotaxis to CXCL12 when compared to unexpanded cells in earlier experiments.

4. Discussion

The key advantages of this novel timelapse assay over existing transwell assays include the ability i) to measure the chemotactic and chemokinetic responses of individual non-adherent progenitor cells for periods comparable to published in vivo homing assays (18–24 h) (Larochelle et al., 2012), ii) to distinguish chemotactic from chemokinetic responses by individual cells to stimuli over time, parameters which are difficult to define in standard transwell assays (Toetsch et al., 2009), iii) to directly compare the strength or response to different or competing stimuli in a single assay, iv) to assess whether stimuli act directly on HSPCs without the complication of niche influences observed in vivo (Shiozawa and Taichman, 2010; Bianco, 2011; Calderón and Boehm, 2012; Park et al., 2012; Psaila et al., 2012), v) to assess small molecule inhibitor effects on individual HSPCs in this multiwell platform for multiple cell migration parameters, and vi) to assess migratory responses of HSPCs in a 3D rather than a 2D environment. A disadvantage is that the substantial data generated in this new assay required manual tracking. When we used Wimasis semi-automated tracking (Khoo et al., 2011), the Wimasis algorithm was unable to follow cells for the duration of the experiment and therefore requires further development.

Using identical CD133$^+$ cells to initiate each assay, the number of human UCB CD133$^+$ cells migrating in the 3D µ-slide chemotaxis assay was 3–5 fold higher than those migrating in the transwell assay (25.9 + 9.2% means + SEM for n = 3 independent experiments). Since the transwell migration results are

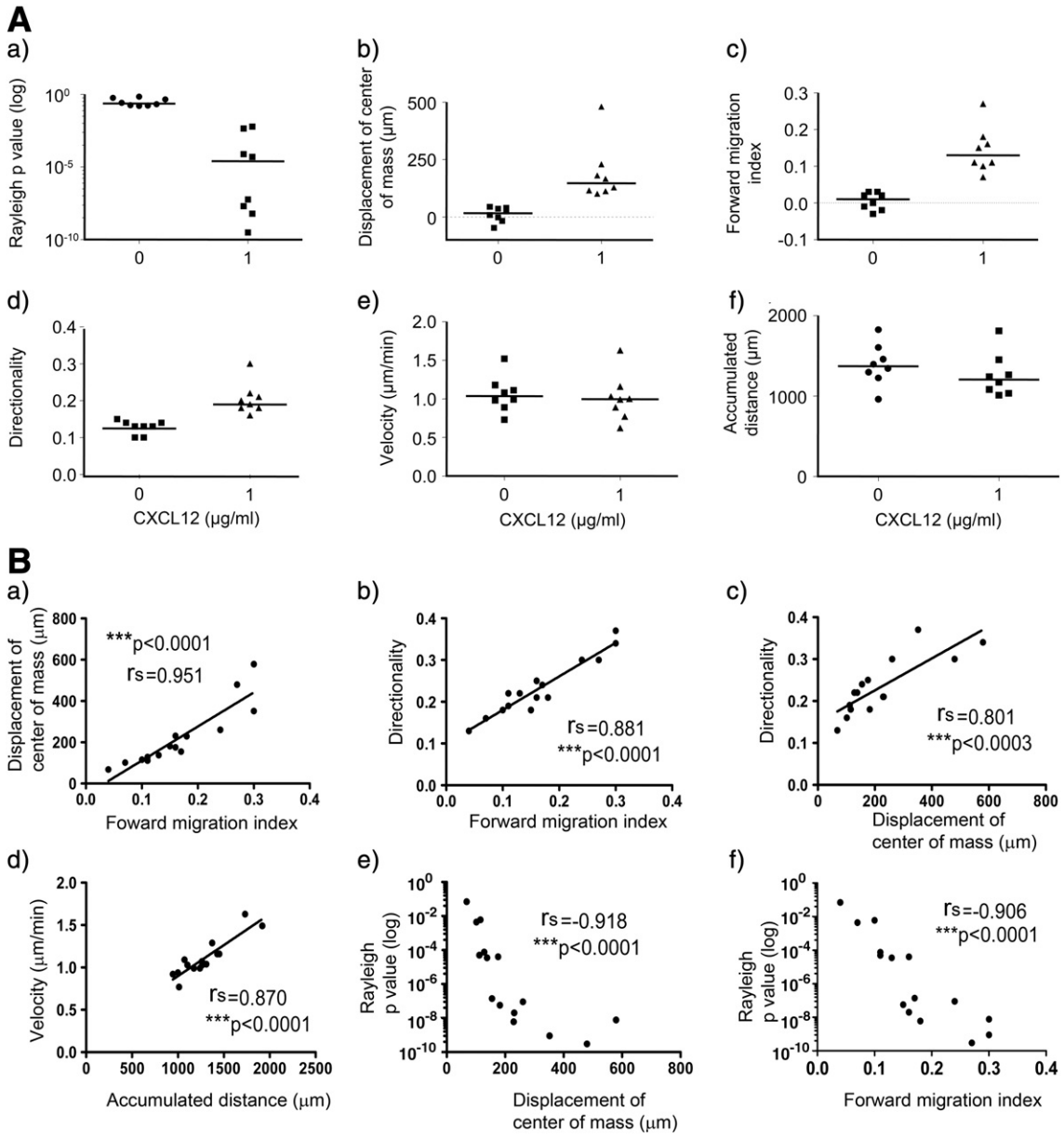

Figure 5 CXCL12 induces human cord blood CD133+ hematopoietic stem/progenitor cell chemotaxis but not chemokinesis. Human UCB CD133+ cells were cultured in StemSpan medium with SCF, Flt-3 ligand, IL-6 and TPO for 24 h, encapsulated in 1 mg/ml collagen I gel and seeded into the central chamber of the 3D chemotaxis μ-slides, prior to adding 0 μg/ml or 1 μg/ml CXCL12 to form a chemokine gradient. (A) The results of 8 independent experiments are displayed as median values (horizontal bar) for individual experiments (scatter plots). Cell migration was tracked using Image J manual tracking software for 22 h and chemotactic and chemokinetic parameters quantified with the chemotaxis and migration tool plug-in for (a) the Rayleigh p value, (b) displacement of the center of mass (blue cross in Figs. 1B and C), (c) forward migration index, (d) directionality, (e) velocity and (f) accumulated distance. Interestingly, there were significant differences in chemotaxis between the chambers containing medium alone and those containing CXCL12, with the following respective changes (mean ± SEM) in Rayleigh values (0.336 ± 0.073 vs. 0.001 ± 0.001; p = 0.0002), displacement of center of mass (10.82 ± 11.25 vs. 189.00 ± 44.26; p = 0.0002) and forward migration index (0.015 ± 0.008 vs. 0.126 ± 0.024; p = 0.0004) over 8 independent experiments, but no significant difference in cell velocity or accumulated distance without or with a CXCL12 gradient (p = 0.7128 and p = 0.2345 respectively). Statistics for chemotactic and chemokinetic data were calculated using the Mann–Whitney test with *$p < 0.05$, **$p < 0.01$ and ***$p < 0.001$. (B) Correlation between (a) displacement of the center of mass and forward migration index, (b,c) directionality and forward migration index or displacement of the center of mass, (d) velocity and accumulated distance, and (e,f) p values of the Rayleigh test and displacement of the center of mass or forward migration index in the presence of a CXCL12 gradient in the 3D μ-slide chemotaxis assay was determined using Spearman's rank correlation coefficient, r_s. p values of *$p < 0.05$, **$p < 0.01$, and ***$p < 0.001$ show significance for n = 15 independent experiments.

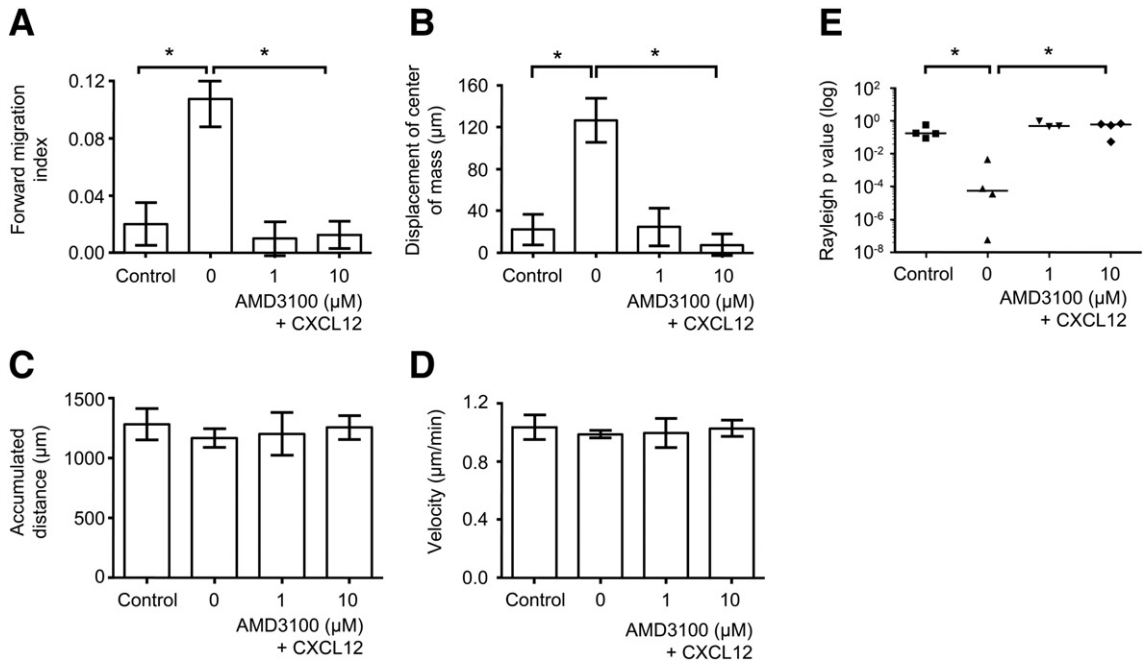

Figure 6 AMD3100 inhibits chemotaxis but not chemokinesis. Human UCB CD133$^+$ cells were cultured in StemSpan medium with SCF, Flt-3 ligand, IL-6 and TPO for 24 h, encapsulated in 1 mg/ml collagen I gel and seeded into the central chamber of the 3D chemotaxis μ-slides, prior to adding 1 μg/ml CXCL12 to form a chemokine gradient with or without AMD3100. Histograms Illustrate the effect of adding 0, 1 μM or 10 μM AMD3100 with 1 μg/ml CXCL12 for the chemotactic or chemokinetic responses of forward migration index (A) and displacement of the center of mass (B) or velocity (C) and accumulated distance (D). Controls contained media alone. Values are means ± SEM for $n \geq 3$ independent experiments. Notably, with the addition of AMD3100, there was a significant decrease in the Rayleigh test p values (E), in displacement of the center of mass (mean ± SEM values of 126.5 μm ± 21.1 for no AMD3100 to 24.7 μm ± 18.1 for 1 μM AMD3100 and 7.5 μm ± 10.6 for 10 μM AMD3100) and in forward migration index (mean ± SEM values of 0.11 ± 0.02 with no AMD3100 and 0.01 ± 0.01 for 1 μM AMD3100 and 0.01 ± 0.01 for 10 μM AMD3100) towards CXCL12 compared to absent AMD3100 ($p < 0.05$ for all). There was no reduction in chemokinesis in terms of the accumulated distance (1167 ± 79 μm) nor the velocity (1.0 ± 0.0 μm/min) of cells without or with AMD3100 addition (1200 ± 179 μm and 1.0 ± 0.1 μm/min respectively for 1 μM AMD3100 and 1255 ± 100 μm and 1.0 ± 0.1 μm/min respectively for 10 μM AMD3100; $p > 0.5$). Statistics were calculated using the Mann–Whitney test with *$p < 0.05$ being significant.

consistent with those described previously (Aiuti et al., 1997; Kim and Broxmeyer, 1998; Kollet et al., 2002; Forde et al., 2007), the differences may be explained by 3D migration in collagen I versus 2D migration on fibronectin, different endpoint times and in situ tracking of migrating cells rather than the need to recover cells prior to analyses. Renkawitz and Sixt (2010) have described plasticity in cell migratory mechanisms in vitro when 3D is compared with 2D environments. Using the 3D assay, we demonstrated increasing cell migration towards CXCL12 over 18 to 22 h of between 67% and 97% of the cells, indicating that these cells do not stop responding to CXCL12 in the 3D environment within the 4–6 hour timeframe used for the 2D transwell assay. In developing this new assay, the weak adhesion of human UCB HSPCs to ECM coated surfaces did not, in our hands, provide an optimal platform for use of the Ibidi 2D μ slide chemotaxis assay. When we attempted to reproduce the 2D μ-slide chemotaxis assay of Grassinger et al. (2009), where the cells were not encapsulated in a matrix, we found that the cells were not easily retained in the observation chamber when the reservoirs were filled. While HSPCs are known to bind to fibronectin through $\alpha_4\beta_1$ and $\alpha_5\beta_1$ integrins (Ulyanova et al., 2011 and references therein), they do not express significant levels of the collagen receptors, $\alpha_1\beta_1$, $\alpha_2\beta_1$, $\alpha_3\beta_1$, $\alpha_{10}\beta_1$, and $\alpha_{11}\beta_1$ (Humphries et al., 2006) and hence this may also affect the mechanics of each assay.

Importantly using CXCL12/CXCR4 interactions as a paradigm for other factors and receptors, we demonstrated that CXCL12 is required for chemotaxis, but not chemokinesis of human UCB CD133$^+$ HSPCs in the absence of niche elements, and that the CXCR4 antagonist, AMD3100, inhibits chemokine sensing but not the ability of these cells to move randomly. This disputes previous suggestions by Entschladen et al. (2005) that chemotaxis does not occur without increasing chemokinesis, and provides a means to study in much more detail the effect of chemokines such as CXCL12 on inducing chemotaxis and/or chemokinesis in leukemic cell lines and primary leukemic stem/progenitor cells (Zepeda-Moreno et al., 2012). Other studies examining the chemotactic and chemokinetic movement of other cell types, such as the HT-1080 carcinoma cell line and human umbilical vein endothelial cells (HUVECs) towards an FCS gradient (Zengel et al., 2011), have demonstrated using Ibidi chemotaxis slides that chemokinetic migration as measured by cell velocity and accumulated distance can be influenced by the presence of a stimulus.

We also examined the effects of short term (8 day) expansion of human UCB CD133$^+$ cells on a cell free nanofiber scaffold in the presence of cytokines on their chemotactic and chemokinetic responses to CXCL12. Using identical human UCB CD133$^+$ cells to initiate the cultures, a greater and consistent expansion of CD133$^+$CD34$^+$ cells was also seen after 8 days in

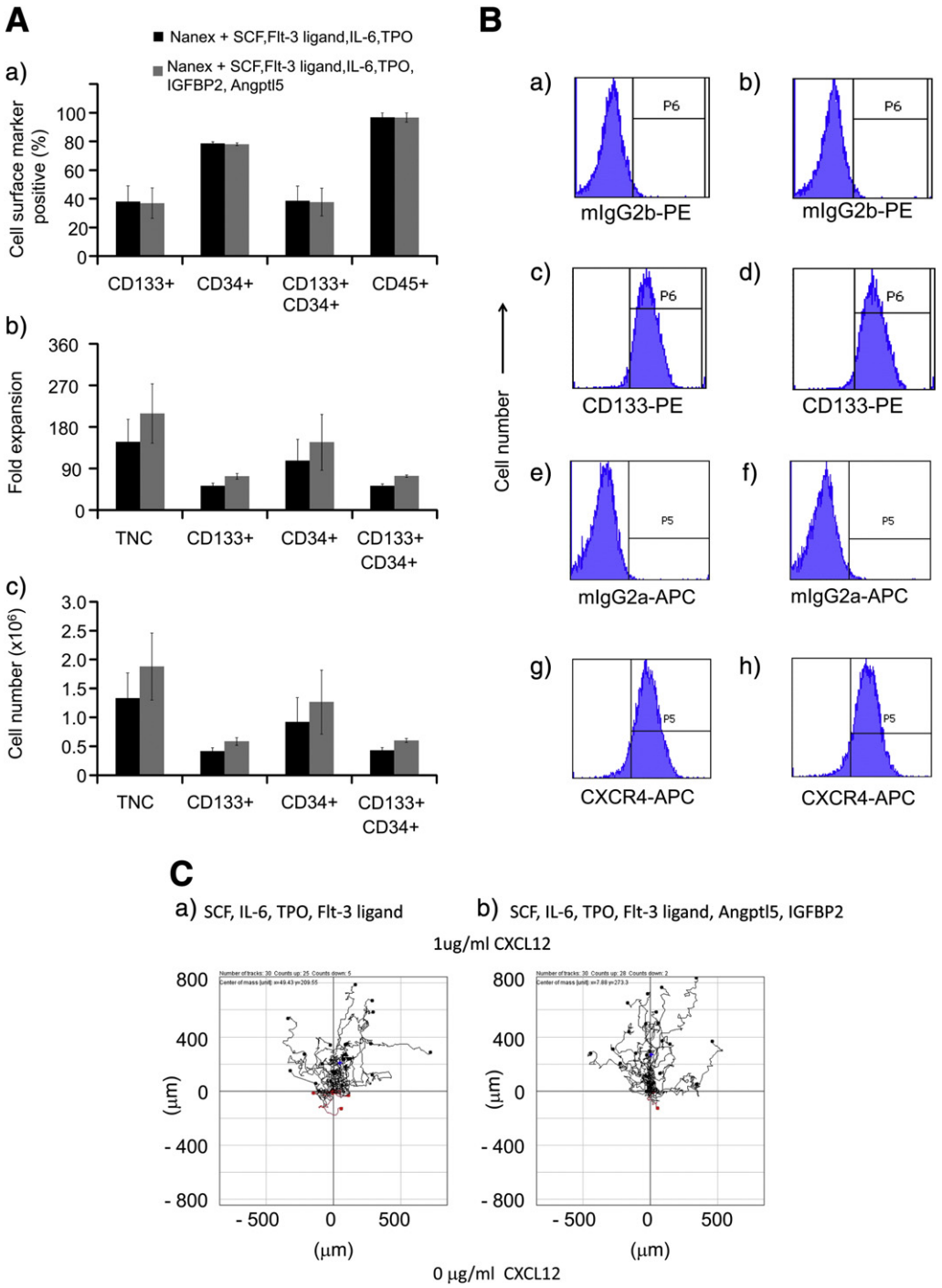

Figure 7 Chemotaxis after cord blood CD133+ cell expansion. Human UCB CD133+ cells were cultured on Nanex nanofiber scaffolds in Nanex serum free HSC expansion medium containing SCF, Flt-3 ligand, IL-6 and TPO without (black histograms) or with (gray histograms) IGFBP2 and Angptl5 for 8 days prior to (A) flow cytometric analyses of surface markers or cell viability or (B) reselecting CD133+ cells and analyzing (C) their chemotactic or chemokinetic responses to CXCL12. The red and black lines indicate whether the cells finished their migration path below or above (towards 1 μg/ml CXCL12) their starting point on the x axis. The Rayleigh p values indicate that there was a significant inhomogeneous distribution of the cells following expansion in either cocktail towards CXCL12 in the presence of a CXCL12 gradient ((a) $p = 3.6 \times 10^{-5}$ and (b) $p = 2.4 \times 10^{-8}$). A(a) shows the % of expanded cells expressing CD133, CD34 and CD45. A(b) shows the fold expansion of TNC and CD133 and CD34 single and dual positive subsets after 8 days of culture. A(c) shows the relative cell numbers generated after 8 day cultures for TNC and each specified cell subset, initiated with 3×10^6 TNC which were 88.4 ± 2.8% CD133+. Values are means + SEM for n = 3 experiments. D shows a comparison of chemotactic and chemokinetic responses of UCB CD133+ cells after 8 days expansion with specific cytokines compared to 24 hour treatment with specific cytokines.

D

Comparison of Chemotactic and Chemokinetic Responses to CXCL12 after Cytokine Stimulation

Parameter	Day 8 Nanex nanofiber scaffold expansion +SCF, Flt-3 ligand, IL-6, TPO*		Day 8 Nanex nanofiber expansion scaffold +SCF, Flt-3 ligand, IL-6, TPO, IGFBP2, Angptl5*		Day 1 StemSpan medium culture +SCF, Flt-3 ligand, IL-6, TPO**	
CXCL12 (μg/ml)	0	1	0	1	0	1
Forward Migration Index	0.027±0.024	0.160±0.025	0.027±0.024	0.173±0.061	0.014±0.009	0.139±0.024
Displacement of Center of Mass (μm)	32.4±14.7	205.9±60.8	32.4±14.7	242.1±18.6	19.0±11.3	182.6±46.0
Velocity (μm/min)	0.97±0.10	0.97±0.10	0.97±0.10	1.00±0.10	1.07±0.08	1.04±0.11
Accumulated Distance (μm)	1215±158	1210±186	1215±158	1177±143	1427±71	1314±91

*n=3 independent experiments using the same batches of UCB $CD133^+$ cells:
** n= 8 independent experiments

Figure 7 (*continued*).

our cultures with the addition of IGFBP2 and Angptl5 to SCF, Flt-3 ligand, IL-6 and TPO than without (averaging 73 versus 52 fold respectively). Drake et al. (2011) using Angptl5 and IGFBP2 together with SCF, TPO and FGF-1 in StemSpan media without a nanofiber scaffold, demonstrated on average a 21 fold increase in $CD133^+CD34^+$ cells after 10 days and a much more variable response between expansion rates than observed here, suggesting that the Nanex scaffold and media used here could be enhancing expansion by greater than 2–3 fold over a shorter period of time. Although Drake et al. (2011) showed that $CD133^+CD34^+$ cell number correlates with repopulating ability in NSG mice, we have yet to demonstrate this. However, when we isolated the $CD133^+$ cells from our expansion cultures and tested their chemotactic response to CXCL12 in the 3D μ-slide chemotaxis assay, we found a non-significant trend towards enhanced chemotaxis but not chemokinesis with the addition of IGBP2 and Angptl5, with these cells continuing to express CXCR4. The 8 day culture did not compromise the chemotactic ability of the expanded $CD133^+$ cells compared to our other experiments where $CD133^+$ cells were cultured for 24 h in SCF, Flt-3 ligand, IL-6 and TPO.

5. Conclusions

In conclusion, this novel 3D μ-slide chemotaxis assay provides a much improved tool, enabling the user to observe the exact response over time of individual HSPCs to chemotactic versus chemokinetic stimuli in vitro, while using fewer cells than standard transwell migration assays. This is an important advance when analyzing rare stem/progenitor cell populations from donors or for use in patients. This 3D μ-slide chemotaxis assay has the added advantage that it can be further extended by using fluorescence microscopy to provide detailed information on heterogeneous populations as well as to examine cell morphology, interactions, division and death, and all cells can be tracked if required. This will complement studies in vivo aimed at the better development of protocols to enhance HSPC expansion, engraftment and mobilization.

Supplementary data to this article can be found online at http://dx.doi.org/10.1016/j.scr.2013.04.006.

Acknowledgments

This work was supported by research funding from the NHS Blood and Transplant (EEP, SMW), the Technology Strategy Board (SMW) and the National Institutes of Health Research (EEP, SMW). This report presents independent research commissioned by the National Institutes for Health Research (NIHR) under its Programme Grants Scheme (RP-PG-0310-1003). The views expressed in this publication are those of the authors and not necessarily those of the NHS, the NIHR or the Department of Health. We would like to thank Ibidi GmbH for providing prototypes of the 3D μ-slide

chemotaxis while they were being developed and for permission to use or reproduce images in Fig. 1. We would also like to acknowledge Arteriocyte Inc. and their distributor, Cambridge Biosciences, for the provision of samples of Nanex plates and media. We thank Mrs. S. Britt and Mrs. J. Walton for collecting the cord blood units.

Authorship contributions

EEP developed the 3D assay, conducted the experimental work and collected the data. EEP and SMW designed, analyzed and reviewed the experimental work and data and wrote and revised the manuscript. SMW obtained the funding.

Disclosure of conflicts of interest

The authors declare no conflicts of interest.

References

Aiuti, A., Webb, I.J., Bleul, C., Springer, T., Gutierrez-Ramos, J.C., 1997. The chemokine SDF-1 is a chemoattractant for human CD34$^+$ hematopoietic progenitor cells and provides a new mechanism to explain the mobilization of CD34$^+$ progenitors to peripheral blood. J. Exp. Med. 185, 111–120.

Aljitawi, O.S., 2012. Ex vivo expansion of umbilical cord blood: where are we? Int. J. Hematol. 95, 371–379.

Bianco, P., 2011. Bone and the hematopoietic niche: a tale of two stem cells. Blood 117, 5281–5288.

Bonig, H., Papayannopoulou, T., 2013. Hematopoietic stem cell mobilization: updated conceptual renditions. Leukemia 27, 24–31.

Broxmeyer, H.E., 2012. Enhancing engraftment of cord blood cells via insight into the biology of stem/progenitor cell function. Ann. N. Y. Acad. Sci. 1266, 151–160.

Calderón, L., Boehm, T., 2012. Synergistic, context-dependent, and hierarchical functions of epithelial components in thymic microenvironments. Cell 149, 159–172.

Christopherson II, K.W., Frank, R.R., Jagan, S., Paganessi, L.A., Gregory, S.A., Fung, H.C., 2012. CD26 protease inhibition improves functional response of unfractionated cord blood, bone marrow, and mobilized peripheral blood cells to CXCL12/SDF-1. Exp. Hematol. 40, 945–952.

Csaszar, E., Kirouac, D.C., Yu, M., Wang, W., Qiao, W., Cooke, M.P., Boitano, A.E., Ito, C., Zandstra, P.W., 2012. Rapid expansion of human hematopoietic stem cells by automated control of inhibitory feedback signaling. Cell Stem Cell 10, 218–229.

Dahlberg, A., Delaney, C., Bernstein, I.D., 2011. Ex vivo expansion of human hematopoietic stem and progenitor cells. Blood 117, 6083–6090.

Dar, A., Kollet, O., Lapidot, T., 2006. Mutual, reciprocal SDF-1/CXCR4 interactions between hematopoietic and bone marrow stromal cells regulate human stem cell migration and development in NOD/SCID chimeric mice. Exp. Hematol. 34, 967–975.

Drake, A.C., Khoury, M., Leskov, I., Iliopoulou, B.P., Fragoso, M., Lodish, H., Chen, J., 2011. Human CD34$^+$ CD133$^+$ hematopoietic stem cells cultured with growth factors including Angptl5 efficiently engraft adult NOD-SCID IL2r$\gamma^{-/-}$ (NSG) mice. PLoS One 6, e18382.

Entschladen, F., Drell IV, T.L., Lang., K., Masur, K., Palm, D., Bastian, P., Niggemann, B., Zaenker, K.S., 2005. Analysis methods of human cell migration. Exp. Cell Res. 307, 418–426.

Forde, S., Tye, B.J., Newey, S.E., Roubelakis, M., Smythe, J., McGuckin, C.P., Pettengell, R., Watt, S.M., 2007. Endolyn (CD164) modulates the CXCL12-mediated migration of umbilical cord blood CD133$^+$ cells. Blood 109, 1825–1833.

Goessling, W., Allen, R., Guan, X., Jin, P., Uchida, N., Dovey, M., Harris, J.M., Metzger, M.E., Bonifacino, A.C., Stroncek, D., Stegner, J., Armant, M., Schlaeger, T., Tisdale, J.F., Zon, L.I., Donahue, R.E., North, T.E., 2011. Prostaglandin E2 enhances human cord blood stem cell xenotransplants and shows long-term safety in preclinical nonhuman primate transplant models. Cell Stem Cell 8, 445–458.

Grassinger, J., Haylock, D.N., Storan, M.J., Haines, G.O., Williams, B., Whitty, G.A., Vinson, A.R., Be, C.L., Li, S., Sørensen, E.S., Tam, P.P., Denhardt, D.T., Sheppard, D., Choong, P.F., Nilsson, S.K., 2009. Thrombin-cleaved osteopontin regulates hemopoietic stem and progenitor cell functions through interactions with $\alpha9\beta1$ and $\alpha4\beta1$ integrins. Blood 114, 49–59.

Hartmann, T.N., Grabovsky, V., Pasvolsky, R., Shulman, Z., Buss, E.C., Spiegel, A., Nagler, A., Lapidot, T., Thelen, M., Alon, R., 2008. A crosstalk between intracellular CXCR7 and CXCR4 involved in rapid CXCL12-triggered integrin activation but not in chemokine-triggered motility of human T lymphocytes and CD34$^+$ cells. J. Leukoc. Biol. 84, 1130–1140.

Hoggatt, J., Pelus, L.M., 2011. Many mechanisms mediating mobilization: an alternative review. Curr. Opin. Hematol. 18, 231–238.

Humphries, J.D., Byron, A., Humphries, M.J., 2006. Integrin ligands at a glance. J. Cell Sci. 119, 3901–3903.

Khoo, C.P., Micklem, K., Watt, S.M., 2011. A comparison of methods for quantifying angiogenesis in the matrigel assay in vitro. Tissue Eng Part C Methods 17, 895–906.

Kim, C.H., Broxmeyer, H.E., 1998. In vitro behavior of hematopoietic progenitor cells under the influence of chemoattractants: stromal cell-derived factor-1, steel factor, and the bone marrow environment. Blood 91, 100–110.

Kollet, O., Petit, I., Kahn, J., Samira, S., Dar, A., Peled, A., Deutsch, V., Gunetti, M., Piacibello, W., Nagler, A., Lapidot, T., 2002. Human CD34($^+$)CXCR4($^-$) sorted cells harbor intracellular CXCR4, which can be functionally expressed and provide NOD/SCID repopulation. Blood 100, 2778–2786.

Kolonin, M.G., Simmons, P.J., 2009. Combinatorial stem cell mobilization. Nat. Biotechnol. 27, 252–253.

Larochelle, A., Gillette, J.M., Desmond, R., Ichwan, B., Cantilena, A., Cerf, A., Barrett, A.J., Wayne, A.S., Lippincott-Schwartz, J., Dunbar, C.E., 2012. Bone marrow homing and engraftment of human hematopoietic stem and progenitor cells is mediated by a polarized membrane domain. Blood 119, 1848–1855.

Lawal, R.A., Calvi, L.M., 2011. The niche as a target for hematopoietic manipulation and regeneration. Tissue Eng. B Rev. 17, 415–422.

Mazo, I.B., Massberg, S., von Andrian, U.H., 2011. Hematopoietic stem and progenitor cell trafficking. Trends Immunol. 32, 493–503.

Mercier, F.E., Ragu, C., Scadden, D.T., 2011. The bone marrow at the crossroads of blood and immunity. Nat. Rev. Immunol. 12, 49–60.

Mohty, M., Ho, A.D., 2011. In and out of the niche: perspectives in mobilization of hematopoietic stem cells. Exp. Hematol. 39, 723–729.

Nagasawa, T., Omatsu, Y., Sugiyama, T., 2011. Control of hematopoietic stem cells by the bone marrow stromal niche: the role of reticular cells. Trends Immunol. 32, 315–320.

Naumann, U., Cameroni, E., Pruenster, M., Mahabaleshwar, H., Raz, E., Zerwes, H.G., Rot, A., Thelen, M., 2010. CXCR7 functions as a scavenger for CXCL12 and CXCL11. PLoS One 5, e9175.

Park, D., Sykes, D.B., Scadden, D.T., 2012. The hematopoietic stem cell niche. Front. Biosci. 17, 30–39.

Peled, A., Petit, I., Kollet, O., Magid, M., Ponomaryov, T., Byk, T., Nagler, A., Ben-Hur, H., Many, A., Shultz, L., Lider, O., Alon, R., Zipori, D., Lapidot, T., 1999. Dependence of human stem cell engraftment and repopulation of nod/scid mice on CXCR4. Science 283, 845–848.

Petrie, R.J., Doyle, A.D., Yamada, K.M., 2009. Random versus directionally persistent cell migration. Nat. Rev. Mol. Cell Biol. 10, 538–549.

Petropoulou, A.D., Rocha, V., 2011. Risk factors and options to improve engraftment in unrelated cord blood transplantation. Stem Cells Int. 2011, 610514.

Psaila, B., Lyden, D., Roberts, I., 2012. Megakaryocytes, malignancy and bone marrow vascular niches. J. Thromb. Haemost. 10, 177–188.

Ramirez, P., Wagner, J.E., DeFor, T.E., Blazar, B.R., Verneris, M.R., Miller, J.S., McKenna, D.H., Weisdorf, D.J., McGlave, P.B., Brunstein, C.G., 2012. Factors predicting single-unit predominance after double umbilical cord blood transplantation. Bone Marrow Transplant. 47, 799–803.

Renkawitz, J., Sixt, M., 2010. Mechanisms of force generation and force transmission during interstitial leukocyte migration. EMBO Rep. 11, 744–750.

Schiraldi, M., Raucci, A., Muñoz, L.M., Livoti, E., Celona, B., Venereau, E., Apuzzo, T., De Marchis, F., Pedotti, M., Bach, i A., Thelen, M., Varan, i.L., Mellado, M., Proudfoot, A., Bianchi, M.E., Uguccioni, M., 2012. HMGB1 promotes recruitment of inflammatory cells to damaged tissues by forming a complex with CXCL12 and signaling via CXCR4. J. Exp. Med. 209 (3), 551–563.

Sharma, M., Afrin, F., Satija, N., Tripathi, R.P., Gangenahalli, G.U., 2011. Stromal-derived factor-1/CXCR4 signaling: indispensable role in homing and engraftment of hematopoietic stem cells in bone marrow. Stem Cells Dev. 20, 933–946.

Shiozawa, Y., Taichman, R.S., 2010. Dysfunctional niches as a root of hematopoietic malignancy. Cell Stem Cell 6, 399–400.

Sun, X., Cheng, G., Hao, M., Zheng, J., Zhou, X., Zhang, J., Taichman, R.S., Pienta, K.J., Wang, J., 2010. CXCL12/CXCR4/CXCR7 chemokine axis and cancer progression. Cancer Metastasis Rev. 29, 709–722.

Toetsch, S., Olwell, P., Prina-Mello, A., Volkov, Y., 2009. The evolution of chemotaxis assays from static models to physiologically relevant platforms. Integr. Biol. (Camb.) 1, 170–181.

Ulyanova, T., Jiang, Y., Padilla, S., Nakamoto, B., Papayannopoulou, T., 2011. Combinatorial and distinct roles of α5 and α4 integrins in stress erythropoiesis in mice. Blood 117, 975–985.

Watt, S.M., 2011. Umbilical cord blood stem cell banking, In: Moo-Young, M., Butler, M., Webb, C., Moreira, A., Grodzinski, B., Cui, Z.F., Agathos, S. (Eds.), Comprehensive Biotechnology, 2nd edition. Elsevier BV Press, Amsterdam, The Netherlands, pp. 397–406.

Watt, S.M., Forde, S.P., 2008. The central role of the chemokine receptor, CXCR4, in haemopoietic stem cell transplantation: will CXCR4 antagonists contribute to the treatment of blood disorders? Vox Sang. 94, 18–32.

Zengel, P., Nguyen-Hoang, A., Schildhammer, C., Zantl, R., Kahl, V., Horn, E., 2011. μ-Slide chemotaxis: a new chamber for long-term chemotaxis studies. BMC Cell Biol. 12 (1), 21–34 (2011 May 18).

Zepeda-Moreno, A., Saffrich, R., Walenda, T., Hoang, V.T., Wuchter, P., Sánchez-Enríquez, S., Corona-Rivera, A., Wagner, W., Ho, A.D., 2012. Modeling SDF-1-induced mobilization in leukemia cell lines. Exp. Hematol. 40, 666–674.

Zhou, B., Tsaknakis, G., Coldwell, K.E., Khoo, C.P., Roubelakis, M.G., Chang, C.H., Pepperell, E., Watt, S.M., 2012. A novel function for the haemopoietic supportive murine bone marrow MS-5 mesenchymal stromal cell line in promoting human vasculogenesis and angiogenesis. Br. J. Haematol. 157, 299–311.

Zou, Y.R., Kottmann, A.H., Kuroda, M., Taniuchi, I., Littman, D.R., 1998. Function of the chemokine receptor CXCR4 in haematopoiesis and in cerebellar development. Nature 393, 595–599.